HHS Public Access

Author manuscript

Behav Brain Res. Author manuscript; available in PMC 2015 May 19.

Published in final edited form as:

Behav Brain Res. 2013 November 1; 256: 529–536. doi:10.1016/j.bbr.2013.06.001.

A large scale (N = 102) functional neuroimaging study of response inhibition in a Go/NoGo task

Vaughn R. Steele[a,b,e], **Eyal Aharoni**[a,b], **Gillian E. Munro**[a], **Vince D. Calhoun**[a,b,c], **Prashanth Nyalakanti**[a], **Michael C. Stevens**[c,d], **Godfrey Pearlson**[c,d], and **Kent A. Kiehl**[a,b]

[a]The Mind Research Network

[b]University of New Mexico

[c]Yale University School of Medicine

[d]Olin Neuropsychiatry Research Center, Institute of Living

Abstract

We report a functional magnetic resonance imaging (fMRI) study of healthy adult participants who completed a demanding Go/NoGo task. The primary purpose of this study was to delineate the neural systems underlying successful and unsuccessful response inhibition using a large sample (N = 102). We identified a number of regions uniquely engaged during successful response inhibition, including a fronto-parietal network involving the anterior cingulate, supplementary motor areas, lateral and inferior prefrontal regions, and the inferior parietal lobule. Unique hemodynamic activity was also noted in the amygdala and in frontostriatal regions including the inferior frontal gyrus and portions of the basal ganglia. Also, contrasts were defined to explore three variants of hemodynamic response allowing for more specificity in identifying the underlying cognitive mechanisms of response inhibition. Addressing issues raised by prior small sample studies, we identified a stable set of regions involved in successful response inhibition. The present results help to incrementally refine the specificity of the neural correlates of response inhibition.

Keywords

Response inhibition; fMRI; Go/NoGo

1. Introduction

How the brain acts to inhibit undesirable motor actions is a question that has fueled extensive research in both basic and clinical fields. A deeper understanding of the neural mechanisms that underlie successful and unsuccessful response inhibition is of tremendous value for cognitive neuroscience in general and various psychopathological conditions in particular.

[e]Corresponding Author during review process: Mobile MRI Core and Clinical Cognitive Neuroscience, The Mind Research Network, University of New Mexico, 1101 Yale Boulevard NE, Albuquerque, NM 87106. Phone: (505) 504-0182. Fax: (505) 272-8002. vsteele@unm.edu.

Several types of inhibition tasks have been employed to examine response inhibition and error processing (e.g, Go/NoGo, Stroop, Stop-signal, Flanker, Wisconsin Card Sorting Task, and Task-Switcthing: see [1] for review). One of the more common paradigms is the Go/NoGo task. In Go/NoGo paradigms, participants are serially presented with targets (Go Stimuli) and distractors (NoGo stimuli) on a computer screen. They are instructed to depress a button whenever they see a target and not when they see a distractor. The ratio of Go vs NoGo trials can be manipulated to create pre-potent response bias towards one or the other stimulus. When Go trials are more frequent than NoGo trials, successful performance requires not just the ability to process response errors per se, but also an ability to withhold or inhibit a pre-potent Go response during NoGo trials. The pre-potent Go/NoGo task is well suited to distinguish between the response inhibition and error processing systems of the brain.

Neuroscience research has identified a number of brain areas responsible for successful response inhibition (see [2]). This network includes the lateral and ventrolateral prefrontal cortex [3–6], inferior frontal gyrus [7–11], inferior parietal lobe [3, 5, 8–10, 12, 13], pre-supplementary motor areas [14], anterior cingulate cortex (ACC; [5, 8, 15]), occipital regions such as the cuneus [5, 16, 17], and subcortical regions including the thalamus and basal ganglia [8, 10, 12, 13, 18–20].

Although there is a growing body of evidence supporting the involvement of the regions discussed above from imaging and lesion studies [21–24], findings across studies are somewhat inconsistent and perhaps misleading [25]. The variability in results may be due to small sample sizes (addressed well in meta analyses [1, 2, 26]) and specificity in relative directionality of the hemodynamic response. Though more recent studies have been published with slightly larger samples ([14, 27–30], N's > = 40), previous studies of response inhibition typically used small sample sizes ([3–5, 9, 12, 31–38] N's < 25). Studies with larger sample sizes ([29, 30] where N = 50) have tended to use different methods, making direct comparison to classical inhibition studies difficult. Small sample sizes are known to hamper the ability to detect small effects (Type II error) in functional neuroimaging studies (see [26, 39, 40]). Combined with a traditional methodological approach, samples large enough to detect small effects (N > 20 as suggested by [26] or N > 24 as suggested by [40]) could potentially address some of the inconsistencies between studies employing classical inhibition tasks and could possibly identify other areas important in response inhibition that may be undetectable in studies with small samples.

Another limitation of the existing neuroimaging of response inhibition is lack of sensitivity to the relative directionality of the hemodynamic response. A traditional contrast examining two conditions (i.e., A and B) can result in at least three possible hemodynamic variants: (Variant 1; RED) condition A has as a large positive response relative to condition B's smaller response of the same direction; (Variant 2; GREEN) condition A has a positive response while condition B has a negative response, and (Variant 3; BLUE) condition A has a small negative response relative to condition B's large negative response (see Figure 1). These three response types likely reflect different information processes in the brain and therefore highlight that not all interpretations of traditional contrasts are equal. For instance, increased positive activation may be more strongly associated with early learning of a task

whereas highly trained task performance may reflect a process of neural specialization that involves the deactivation of regions that are no longer needed for successful task performance (see [41, 42]). Most studies employing fMRI have not focused on the relative directionality of the hemodynamic response and have focused only on identifying significant differences, regardless of the variant. By typing the hemodynamic response into these three variants within each contrast, we can get closer to understanding the complex nature of the cognitive mechanisms underlying response inhibition.

We report here an fMRI investigation of 102 participants who completed a difficult Go/NoGo task requiring the response inhibition of a pre-potent response [15]. It was hypothesized that inhibition specific hemodynamic activity measured here would overlap with previously identified regions associated with inhibition (see Table 1). Importantly, with a large sample (N=102), we expected to identify all of previously reported regions associated with response inhibition in this single report. We predict that each of the three variants of hemodynamic activation will identify regions that contribute to task-specific processes, which will allow for a more complex understanding of the neural processes that underlie response inhibition.

2. Methods

2.1. Participants

Participants consisted of 102 healthy adults (49 men) ranging in age from 23 to 52 years (*M* = 33.92, *SD* = 9.64) drawn from the Olin Neuropsychiatry Research Center at the Institute of Living Hartford Hospital and the surrounding community of Hartford, CT via advertisements, presentations at local universities, and word-of-mouth. Seven participants (7%) were left-handed. The sample reflected the ethnic nature of the community: 68% of the sample self-identified as White, 10% as Black/African American, 9% as Hispanic, 8% as Asian, and 6% as Mixed/Other racial heritage. Using the Structured Clinical Interview for the DSM-IV, all participants were free of any history of psychiatric illness (Axis I and II; [43]) and reported no history of psychosis in first-degree relatives. Participants reported they all had normal hearing, and visual acuity was normal or corrected to normal, using contact lenses or MR compatible glasses. Participants provided written informed consent in protocols approved by Institute of Living/Hartford Hospital's Institutional Review Board.

2.2. Experimental Design

Two scanning runs each comprising 245 visual stimuli were presented to participants using a computer-controlled visual and auditory presentation package (VAPP) designed by the senior author. Stimuli were displayed on a rear-projection screen mounted at the rear entrance to the magnet bore and subtended a visual angle of ~3 × 3.5°. Each stimulus appeared for 250 ms in white text within a continuously displayed rectangular fixation box. Participants viewed the screen by means of a mirror system attached to the head coil.

Participants were instructed to respond as quickly and accurately as possible with their right index finger to each presentation of the Go stimulus (the letter 'X'; 412 total trials with the occurrence probability of 0.84). They were instructed to withhold a response to the NoGo stimulus (the letter 'K'; 78 total trials with the occurrence probability of 0.16). Task

difficulty could be attributed to the rapid exposure to rare violations of this response set using stimulus letters close in visual similarity. The relatively high probability of targets was necessary to build a pre-potent response set and elicit a sufficient number of errors to justify their independent examination. Before each run, all participants were encouraged to respond as quickly and accurately as possible. Prior to scanning, participants completed a brief practice session of ~10 trials.

The stimulus onset asynchrony (SOA) between stimuli varied pseudo-randomly between 1000, 2000 and 3000 ms with an average SOA of 1.5 s. No more than three Go stimuli were presented within each consecutive 6 s period. The NoGo stimuli were interspersed among the Go stimuli in a pseudorandom manner subject to three constraints: the minimum SOA between a Go and NoGo stimulus was 1000 ms; the SOA between successive NoGo stimuli was between 8 s and 15 s; and stimuli (both Go and NoGo) had an equal likelihood of occurring at 0, 500 or 1000 ms after the beginning of a 1.5 s acquisition period (TR). By jittering stimulus presentation relative to the acquisition time, the hemodynamic response to the stimuli of interest was sampled effectively at 500 ms intervals.

Behavioral responses were recorded using a commercially available MRI-compatible fiber optic response device (Lightwave Medical, Vancouver, BC). Correct hits, or Hits, were defined as Go ('X' stimuli) trials that were followed by a button press within 1000 ms of stimulus onset. Correctly rejected NoGo trials, or correct rejections (CR), were determined by the absence of a motor response within 1000 ms of the NoGo stimulus. NoGo trials that were followed by a button press within 1000 ms of stimulus onset were defined as false alarms. For simplicity, and to identify the response inhibition neural correlates, only Hits and CR were analyzed.

2.3. Imaging Parameters

Imaging data were collected on a Siemens' Allegra 3T system located at the Olin Neuropsychiatry Research Center, Hartford, CT. Each participant's head was firmly secured using a custom head holder, and head motion was restricted using a custom-built cushion inside the head coil. Localizer images were acquired to determine functional image volumes. The echo planar image (EPI) gradient-echo pulse sequence (TR/TE = 1500/28 ms; flip angle = 65°; FOV = 24 × 24 cm; 64 × 64 matrix; 3.4 × 3.4 mm in plane resolution; 5 mm effective slice thickness; 30 total slices) effectively covered the entire brain (150 mm) in 1.5 s. Each of the two runs lasted just over 7 minutes, or 281 scans. A 9 s rest period was included prior to the start of the task in each run to allow for T_1 effects to stabilize. The six initial images from stabilization period were discarded before post-processing.

2.4. Image Processing

Functional images were reconstructed offline at 16-bit resolution and manually reoriented to approximately the anterior commissure/posterior commissure (AC/PC) plane. Functional image runs were motion corrected using an algorithm unbiased by local signal changes (INRIAlign [44, 45]) as implemented in the SPM2 software [46].

A mean functional image volume was constructed for each run from the realigned image volumes. The mean EPI image was normalized to the EPI template. The spatial

transformation into standard MNI space was determined using a tailored algorithm with both linear and nonlinear components [47]. The normalization parameters determined for the mean functional volume were then applied to the corresponding functional image volumes for each participant. The normalized functional images were smoothed with a 9 mm full width at half-maximum (FWHM) Gaussian filter. Event-related responses were modeled using a synthetic hemodynamic response function composed of two gamma functions. The first gamma function modeled the hemodynamic response using a peak latency of 6 s. A term proportional to the derivative of this gamma function was included to allow for small variations in peak latency. The second gamma function and associated derivative was used to model the small "overshoot" of the hemodynamic response on recovery. High-pass (cutoff period 116 s) and low-pass (cutoff period .23 s) filters were applied to remove any low- and high-frequency confounds, respectively. A latency variation amplitude-correction method was used to provide a more accurate estimate of hemodynamic response for each condition that controlled for differences between slices in timing and variation across regions in the latency of the hemodynamic response [48].

In addition to the traditional hemodynamic response contrast (beta values for condition A > beta values for condition B), three hemodynamic variants were determined by calculating and comparing the beta values for each contrast: (Variant 1; RED) condition A has a large positive response relative to condition B's smaller response of the same direction; (Variant 2; GREEN) condition A has a positive response while condition B has a negative response, and (Variant 3; BLUE) condition A has a small negative response relative to condition B's large negative response (see Figure 1). In each instance, whole-brain analysis was carried out using *t*-test to identify significant differences. This technique provides information about signal directionality and accounts for the time course of the hemodynamic response.

2.5. Data Analytic Strategy

To highlight neural correlates of response inhibition, only CR and Hits will be discussed though the neural processing was initially modeled with all trial types. Following preprocessing of the functional images, first-level general linear model analyses (GLM) included regressors to model correct responses, incorrect responses, and successful inhibitions. Correct hits were designed as a baseline condition on which to compare correctly rejected (NoGo) events allowing us to examine the positively reinforcing events specific to motor inhibition. The comparison of interest was CR events versus Hits. This contrast confounds two different stimulus types (i.e., "X" and "K"); however, both represent correct responses. All contrasts were whole-brain analyses and thresholded 10 extent voxels and *t*-test $p < .05$, corrected for multiple comparisons using the family-wise error (FWE) correction as implemented in SPM.

3. Results

3.1. Behavioral data

Participants averaged 99% correct hits out of total hits and misses (95% CI upper bound = 99.6%), and the mean percentage of false alarms out of total false alarms and correct rejections (CR) was 39% (95% CI upper bound = 41.0%). Average response time (RT) for

Hits was 375 ms (*SD* = 85 ms) and false alarms was 345 ms (*SD* = 69 ms). No gender differences for RT or accuracy were present. Age was positively correlated with RT for Hits ($r = .35$, $p < .001$).

3.2. Imaging data

Response inhibition—Using a traditional hemodynamic contrast (*t*-tests), comparing CR to Hits revealed 36 areas of relative activation, which can be found in Table 2 and Figure 2A. Eta squared was calculated for each of the 36 areas highlighting the variance related to response inhibition within each region of interest (see Table 2). Response inhibition was associated with neural activity in a number of frontal areas, including right orbitofrontal cortex (BA 10), right dorsolateral prefrontal cortex (BA 9), right SMA/pre-SMA (BA 6), bilateral inferior frontal gyrus (BA 47) bordering the insula, and the ACC (BA 24). There was also significantly increased hemodynamic response in a number of other predominantly right-hemisphere regions, including temporal regions (BAs 21, 22, & 37) bilaterally in the inferior parietal lobule (BA 40), regions of the striatum and cerebellum, and regions of the occipital lobe (BA 18, 19, & 30), including the cuneus. This traditional contrast is informative in that we were able to identify a group of regions associated with the hemodynamic differences between CR and Hits. However, little information is gained towards an understanding of the relative activation of the conditions. Using the hemodynamic variants discussed above, more detailed information about relative activations was apparent (see Figure 2B). All regions identified in the traditional contrast exhibited a positive hemodynamic response of CR relative to a smaller positive response to Hits (Variant 1; RED) except for the cuneus, whose CR response was less negative than in Hits (Variant 3; BLUE), and the precuneus, whose CR response was positive relative to a negative response in Hits (Variant 2; GREEN). The SPM toolbox Marsbar was used to extract regions of interest within each of these three variants (see Table 3).

Analyses using a median split of response time to Hits (fast vs slow) and False Alarm rates (good vs poor inhibitors) did not identify specific regions unique to behavioral processes other than response inhibition. Similarly, a correlation between False Alarm rates and neural activity did not prove significant. Though these behavioral differences have been demonstrated previously in fMRI [49] and event-related potentials (ERPs; [50, 51]), the modeling procedure employed here took into consideration the latency related to amplitude differences in hemodynamic response (for full details, see [52]) to ensure the most accurate measurement controlling for latency jitter (as might be found between fast and slow responses to Hits). Neither age nor gender was correlated with the neural measures presented here. Additionally, interactions of task related activations with gender and age we carried out. A two-sample *t*-test was computed to compare males and females and a regression model was used to measure age related differences. Neither age nor gender proved to interact with the above findings.

4. Discussion

This study recorded event-related fMRI associated with response inhibition during a Go/NoGo task. Response inhibition, as explored via trials in which NoGo stimuli were correctly rejected relative to Go stimuli with correct responses, was associated with neural activity in

a large number of brain regions, including inferior, lateral and medial frontal areas, temporal cortex, inferior parietal lobe, occipital lobe and subcortical regions. This study represented the first large-scale (N > 100) imaging examination of response inhibition (see [26, 39, 40] for discussions of benefits of large sample size in GLM analysis of fMRI). In a single study, we confirmed the involvement of many regions that had not been consistently found in previous studies using traditional analytic techniques and smaller sample sizes. Table 1 summarizes the degree of correspondence between the present results and those of similar studies despite occasional differences in baseline. We restrict this comparison to GLM-based fMRI studies of inhibition in healthy adults performing a Go/NoGo task (see Table 1). By using traditional and new hemodynamic variants, we have been able to identify relative activation levels between conditions that allows for a more thorough understanding of the neural correlates of response inhibition.

In regards to successful response inhibition, we noted a wide distribution of active regions in our primary contrast (Correct Rejects vs. Hits). Among these, we observed strong activity in the ACC, consistent with previous research [3, 8, 12, 20, 53]. We also observed activation of occipital regions including the cuneus [5, 16, 17, 54] and precuneus [3, 5, 10, 13, 34]. Engagement of the cuneus has not been consistently observed in Go/NoGo studies employing the GLM, possibly due to limitations in statistical power. However, this region has been identified using independent components analysis (ICA; [29, 30]), a computational method of separating multivariate signals into individual subcomponents. The correspondence between these studies (see Table 1) and the range of effect sizes presented here (see Table 2) attests to the importance of large samples when utilizing GLM techniques to examine response inhibition.

Confirming earlier reports of the involvement of the right-lateralized fronto-parietal network in response inhibition, we also observed activity in bilateral inferior frontal and right inferior parietal regions [3, 4, 8, 9, 11, 55]. Activity in parietal regions has been associated with the motor and attentional control required to inhibit a pre-potent response [9], and such activity increases with the pre-potent tendency to respond [53]. However, similar activity in this network has also been associated with more general cognitive or attentional control functions [14, 33, 56]. For example, although dorsal and ventral lateral prefrontal regions are thought to be an important component in response control, activity in this region is sensitive to task demands[14], and may reflect other processes such as working memory load [14, 56].

It is likely that many frontal regions and networks underlie multiple executive functions [25]. Given that the current Go/NoGo task required minimal working memory, the strong activity noted in BA 9 suggests a unique lateral prefrontal contribution to response inhibition. Likewise, we also noted significant activity in inferior frontal regions [7–9, 12, 57–59]. This area has been uniquely associated with response inhibition [60]. The inferior frontal gyrus is also integral to a frontostriatal circuit [61–63]. These regions have rich reciprocal connections with the basal ganglia, and there are a number of circuits between frontal and striatal regions that could contribute to response inhibition. These regions are also implicated in conditions characterized by impaired response inhibition such as attention deficit/hyperactivity disorder [64], Parkinson’s disease [65], and patients with lesions to the basal ganglia [66, 67]. We found that correctly rejected trials were associated with increased

activity in striatal basal ganglia regions. This result is common among studies using Go/NoGo tasks, reporting increased activity in striatal regions [8, 20, 56, 63].

The second purpose of the current study was to explore differences in hemodynamic response directionality. A broad area of more positive activation associated with CR relative a slightly less positive activation associated with Hits (Variant 1; RED) was observed (Figure 2B). Several of these regions have been highly related to response inhibition (e.g., right dorsal lateral cortex, right SMA/pre-SMA, bilateral inferior frontal gyrus, and ACC; [5, 7–11, 14, 15, 68]). Perhaps the two most interesting findings with respect to these directionality effects are the cuneus and precunues where Hits were more negative than CRs (see Table 3). Though there are previous instances of measuring activation in these regions during response inhibition [5, 16, 17], these regions may not be associated with response inhibition directly. For instance, both the cuneus and precuneus have been linked to consciousness, episodic memory retrieval, and the default mode network [69–72]. The observed hemodynamic variants could potentially be explained by these theories (e.g., a default mode network or inverse workload dependent interpretation would explain greater deactivation in the default mode network for the easier of the two task conditions. In this case, the Hit condition carries less cognitive load and therefore requires less in the way of workload relative to the CR condition). Therefore, to understand contributions of these areas and the relative hemodynamic activations, further explorations of these GREEN and BLUE regions found in figure 2B is necessary. This highlights that knowing the directionality of the hemodynamic response improves reliability assessments of brain areas that appear to be similarly engaged across multiple samples and tasks. This has allowed us to confirm similarities in hemodynamic activations across the right dorsal lateral cortex, right SMA/pre-SMA, bilateral inferior frontal gyrus, and ACC involved in inhibition. Different hemodynamic activations were measured in the cuneus and precuneus during response inhibition than in other regions suggesting the measurement of potentially different cognitive functions, though further exploration is necessary.

As suggested from the results of previous work [8, 18, 20, 56, 62, 63], the interpretation of these Go/NoGo results cannot necessarily be expanded to include other forms of response inhibition, such as the inhibition of already initiated motor-responses seen in stop-signal tasks. For example, we have identified, supported by previous reports [8, 20, 56, 63], increased activity in striatal regions for CRs. In contrast, CR measured during a stop-signal tasks frequently implicate the subthalamic nucleus [18, 62], another region of the basal ganglia. These varied findings could potentially reflect the different demands of the two inhibition tasks (see [73]). A full understanding of response inhibition more generally must consider variations between tasks at least as much as the convergence commonly emphasized within tasks.

Future investigations of the hemodynamic variants outlined here would be necessary to understand the relative contributions to response inhibition. The variants could be linked to separable, transient cognitive mechanisms associated with response inhibition [10, 17, 19, 74] that are best identified with ERPs. Unlike fMRI, with ERPs, it is possible to separate several underling cognitive functions that occur within a single trial. ERPs have been used to measure cognitive functions associated with stimulus processing, response inhibition,

responding (either correctly or incorrectly), and post-response strategy modification within single trial of a Go/NoGo task. Therefore, a combination of the spatial resolution from fMRI and the temporal resolution from ERPs may be necessary to disentangle each of these underlying neural mechanisms. Combining ERPs and fMRI findings with a unique ICA analysis [75] could help elucidate the time course and spatial location of neural activity associated with response inhibition and, more specifically, the hemodynamic variants reported here.

In summary, the results presented here represent one of the largest-sample imaging investigations of response inhibition in a healthy sample conducted to date. Participants were presented with a fast-paced Go/NoGo task, and identified numerous regions that have been inconsistently shown to be engaged using similar methods. Indeed, no other study has reported engagement of the breadth of regions observed here. This speaks to the importance of larger samples in imaging studies that employ GLM techniques. We identified 36 areas associated with response inhibition when correctly rejected NoGo trials were compared with Hits (see Table 2). This is comparable to the number of regions of interest identified in a previous study using 100 participants who completed an auditory oddball task [39]. Aside from identifying regions such as the ACC that are frequently associated with these processes, here we highlighted the advantage of analyzing additional hemodynamic responses to better isolate neural correlates of response inhibition.

Acknowledgments

The authors thank Craig Bennett, Matthew Shane, J. Michael Maurer, Lora Cope, Eric Claus, members of the Olin Neuropsychiatry Research Center, and members of the Mind Research Network. This research was supported in part by grants from the National Institute of Mental Health: 1 R01 MH070539-01 (PI: Kiehl), 1 R01 MH071896-01 (PI: Kiehl), RO1 DA020709 (PI: Pearlson), and P50-AA12870-05 (PI for Project 4: Pearlson).

References

1. Niendam TA, Laird AR, Ray KL, Dean YM, Glahn DC, Carter CS. Meta-analytic evidence for a superordinate cognitive control network subserving diverse executive functions. Cogn Affect Behav Neurosci. 2012; 12:241–68. [PubMed: 22282036]
2. Simmonds DJ, Pekar JJ, Mostofsky SH. Meta-analysis of Go/No-go tasks demonstrating that fMRI activation associated with response inhibition is task-dependent. Neuropsychologia. 2008; 46:224–32. [PubMed: 17850833]
3. Braver TS, Barch DM, Gray JR, Molfese DL, Snyder A. Anterior cingulate cortex and response conflict: Effects of frequency, inhibition, and errors. Cereb Cortex. 2001; 11:825–36. [PubMed: 11532888]
4. Horn NR, Dolan M, Elliott R, Deakin JFW, Woodruff PWR. Response inhibition and impulsivity: An fMRI study. Neuropsychologia. 2003; 41:1959–66. [PubMed: 14572528]
5. Liddle PF, Kiehl KA, Smith AM. Event-related fMRI study of response inhibition. Hum Brain Mapp. 2001; 12:100–9. [PubMed: 11169874]
6. Schulz KP, Fan J, Tang CY, Newcorn JH, Buchsbaum MS, Cheung AM, et al. Response inhibition in adolescents diagnosed with attention deficit hyperactivity disorder during childhood: An event-related fMRI study. American Journal of Psychiatry. 2004; 161:1650–7. [PubMed: 15337656]
7. Aron AR, Robbins TW, Poldrack RA. Inhibition and the right inferior frontal cortex. Trends Cogn Sci. 2004; 8:170–7. [PubMed: 15050513]
8. Garavan H, Ross TJ, Murphy K, Roche RAP, Stein EA. Dissociable executive functions in the dynamic control of behavior: Inhibition, error detection, and correction. Neuroimage. 2002; 17:1820–9. [PubMed: 12498755]

9. Garavan H, Ross TJ, Stein EA. Right hemispheric dominance of inhibitory control: An event-related functional MRI study. Proc Natl Acad Sci U S A. 1999; 96:8301–6. [PubMed: 10393989]
10. Mathalon DH, Whitfield SL, Ford JM. Anatomy of an error: ERP and fMRI. Biol Psychol. 2003; 64:119–41. [PubMed: 14602358]
11. McNab F, Leroux G, Strand F, Thorell L, Bergman S, Klingberg T. Common and unique components of inhibition and working memory: An fMRI, within-subjects investigation. Neuropsychologia. 2008; 46:2668–82. [PubMed: 18573510]
12. Menon V, Adleman NE, White CD, Glover GH, Reiss AL. Error-related brain activation during a Go/NoGo response inhibition task. Hum Brain Mapp. 2001; 12:131–43. [PubMed: 11170305]
13. Wager TD, Sylvester CY, Lacey SC, Nee DE, Franklin M, Jonides J. Common and unique components of response inhibition revealed by fMRI. Neuroimage. 2005; 27:323–40. [PubMed: 16019232]
14. Mostofsky SH, Schaefer JGB, Abrams MT, Goldberg MC, Kraut MA, Denckla MB, et al. fMRI evidence that the neural basis of response inhibition is task-dependent. Cognitive Brain Research. 2003; 17:419–30. [PubMed: 12880912]
15. Kiehl KA, Liddle PF, Hopfinger JB. Error processing and the rostral anterior cingulate: An event-related fMRI study. Psychophysiology. 2000; 37:216–23. [PubMed: 10731771]
16. Garavan H, Ross TJ, Kaufman J, Stein EA. A midline dissociation between error-processing and response-conflict monitoring. Neuroimage. 2003; 20:1132–9. [PubMed: 14568482]
17. Tian Y, Yao D. A study on the neural mechanism of inhibition of return by the event-related potential in the Go/NoGo task. Biol Psychol. 2008; 79:171–8. [PubMed: 18524452]
18. Aron AR. The neural basis of inhibition in cognitive control. The Neuroscientist. 2007; 13:214–28. [PubMed: 17519365]
19. Bekker EM, Kenemans JL, Verbaten MN. Source analysis of the N2 in a cued Go/NoGo task. Cognitive Brain Research. 2005; 22:221–31. [PubMed: 15653295]
20. Garavan H, Hester R, Murphy K, Fassbender C, Kelly C. Individual differences in the functional neuroanatomy of inhibitory control. Brain Res. 2006; 1105:130–42. [PubMed: 16650836]
21. Falkenstein M, Hielscher H, Dziobeck I, Schwarzenau P, Hoorman J, Sundermann B, et al. Action monitoring, error detection, and the basal ganglia: An ERP study. Neuroreport. 2001; 12:157–61. [PubMed: 11201078]
22. Gehring WJ, Knight RT. Prefrontal-cingulate interactions in action monitoring. Nat Neurosci. 2000; 3:516–20. [PubMed: 10769394]
23. Ullsperger M, von Cramon DY. The role of intact frontostriatal circuits in error processing. Journal of Cognitive Neuroscience. 2006; 18:651–64. [PubMed: 16768367]
24. Ullsperger M, von Cramon DY, Müller NG. Interactions of frontal cortical lesions with error processing: Evidence from event-related brain potentials. Neuropsychology. 2002; 16:548–61. [PubMed: 12382993]
25. Criaud M, Boulinguez P. Have we been asking the right questions when assessing response inhibition in go/no-go tasks with fMRI? A meta-analysis and critical review. Neurosci Biobehav Rev. 2013; 37:11–23. [PubMed: 23164813]
26. Murphy K, Garavan H. An empirical investigation into the number of subjects required for an event-related fMRI study. Neuroimage. 2004; 22:879–85. [PubMed: 15193618]
27. Bellgrove MA, Hester R, Garavan H. The functional neuroanatomical correlates of response variability: Evidence from a response inhibition task. Neuropsychologia. 2004; 42:1910–6. [PubMed: 15381021]
28. Rubia K, Smith AB, Woolley J, Nosarti C, Heyman I, Taylor E, et al. Progressive increase of frontostriatal brain activation from childhood to adulthood during event-related tasks of cognitive control. Hum Brain Mapp. 2006; 27:973–93. [PubMed: 16683265]
29. Stevens MC, Kiehl KA, Pearlson GD, Calhoun VD. Functional neural networks underlying response inhibition in adolescents and adults. Behav Brain Res. 2007; 181:12–22. [PubMed: 17467816]
30. Stevens MC, Kiehl KA, Pearlson GD, Calhoun VD. Brain network dynamics during error commission. Hum Brain Mapp. 2009; 30:24–37. [PubMed: 17979124]

31. Altshuler LL, Bookheimer SY, Townsend J, Proenza MA, Eisenberger N, Sabb F, et al. Blunted activation in orbitofrontal cortex during mania: A functional magnetic resonance imaging study. Biol Psychiatry. 2005; 58:763–9. [PubMed: 16310510]
32. Chikazoe J, Jimura K, Asari T, Yamashita K, Morimoto H, Hirose S, et al. Functional dissociation in right inferior frontal cortex during performance of go/no-go task. Cereb Cortex. 2009; 19:146–52. [PubMed: 18445602]
33. Hester RL, Murphy K, Foxe JJ, Foxe DM, Javitt DC, Garavan H. Predicting success: Patterns of cortical activation and deactivation prior to response inhibition. Journal of Cognitive Neuroscience. 2004; 16:776–85. [PubMed: 15200705]
34. Clare-Kelly AM, Hester R, Murphy K, Javitt DC, Foxe JJ, Garavan H. Prefrontal-subcortical dissociations underlying inhibitory control revealed by event-related fMRI. European Journal of Neuroscience. 2004; 19:3105–12. [PubMed: 15182319]
35. Maltby N, Tolin DF, Worhunsky P, O'Keefe TM, Kiehl KA. Dysfunctional action monitoring hyperactivates frontal-striatal circuits in obsessive-compulsive disorder: An event-related fMRI study. Neuroimage. 2005; 24:495–503. [PubMed: 15627591]
36. Nielson KA, Langenecker SA, Garavan H. Differences in the functional neuroanatomy of inhibitory control across the adult life span. Psychology and Aging. 2002; 17:56–71. [PubMed: 11931287]
37. Roth RM, Saykin AJ, Flashman LA, Pixley HS, West JD, Mamourian AC. Event-related functional magnetic resonance imaging of response inhibition in obsessive-compulsive disorder. Biol Psychiatry. 2007; 62:901–9. [PubMed: 17511967]
38. Walther S, Goya-Maldonado R, Stippich C, Weisbrod M, Kaiser S. A supramodal network for response inhibition. Neuroreport. 2010; 21:191–5. [PubMed: 20084035]
39. Kiehl KA, Stevens MC, Laurens KR, Pearlson G, Calhoun VD, Liddle PF. An adaptive reflexive processing model of neurocognitive function: Supporting evidence from a large scale (n = 100) fMRI study of an auditory oddball task. Neuroimage. 2005; 25:899–915. [PubMed: 15808990]
40. Desmond JE, Glover GH. Estimating sample size in functional MRI (fMRI) neuroimaging studies: Statistical power analyses. Journal of Neuroscience Methods. 2002; 118:115–28. [PubMed: 12204303]
41. Brown TT, Lugar HM, Coalson RS, Miezin FM, Petersen SE, Schlaggar BL. Developmental changes in human cerebral functional organization for word generation. Cereb Cortex. 2005; 15:275–90. [PubMed: 15297366]
42. Petersen SE, van Mier H, Fiez JA, Raichle ME. The effects of practice on the functional anatomy of task performance. Proc Natl Acad Sci U S A. 1998; 95:853–60. [PubMed: 9448251]
43. First, MB.; Spitzer, RL.; Gibbon, MWJB.; Williams, JBW. Structured clinical interview for DSM-IV axis I (SCID-I), clinician version. Washington DC: American Psychiatric Press; 1997.
44. Freire L, Mangin JF. Motion correction algorithms may create spurious brain activations in the absence of subject motion. Neuroimage. 2001; 14:709–22. [PubMed: 11506543]
45. Freire L, Roche A, Mangin JF. What is the best similarity measure for motion correction in fMRI time series? IEEE Transactions on Medical Imaging. 2002; 21:470–84. [PubMed: 12071618]
46. Wellcome Trust Centre for Neuroimaging UCL.
47. Friston KJ, Holmes AP, Worsley KJ, Poline J-P, Frith CD, Frackowiak RSJ. Statistical parametric maps in functional imaging: A general linear approach. Hum Brain Mapp. 1994; 2:189–210.
48. Calhoun VD, Kiehl KA, Liddle PF, Pearlson GD. Aberrant localization of synchronous hemodynamic activity in auditory cortex reliably characterizes schizophrenia. Biol Psychiatry. 2004; 55:842–9. [PubMed: 15050866]
49. Hester R, Fassbender C, Garavan H. Individual differences in error processing: A review and reanalysis of three event-related fMRI sudies using the go/nogo task. Cereb Cortex. 2004; 14:986–94. [PubMed: 15115734]
50. de Bruijn ER, Miedl SF, Bekkering H. Fast responders have blinders on: ERP correlates of response inhibition in competition. Cortex. 2008; 44:580–6. [PubMed: 18387590]

51. Falkenstein M, Hoorman J, Hohnsbein J. ERP components in Go/Nogo tasks and their relation to inhibition. Acta Neuropsychiatrica. 1999; 101:267–91.
52. Calhoun VD, Stevens MC, Pearlson GD, Kiehl KA. fMRI analysis with the general linear model: Removal of latency-induced amplitude bias by incorporation of hemodynamic derivative terms. Neuroimage. 2004; 22:252–7. [PubMed: 15110015]
53. Durston S, Thomas KM, Worden MS, Yang Y, Casey BJ. The effect of preceding context on inhibition: An event-related fMRI study. Neuroimage. 2002; 16:449–53. [PubMed: 12030830]
54. Braet W, Johnson KA, Tobin CT, Acheson R, Bellgrove MA, Robertson IH, et al. Functional developmental changes underlying response inhibition and error-detection processes. Neuropsychologia. 2009; 47:3143–51. [PubMed: 19651151]
55. de Zubicaray GI, Andrew C, Zeyala FO, Williams SCR, Dumanoir C. Motor response suppression and the prepotent tendency to respond: A parametric fMRI study. Neuropsychologia. 2000; 38:1280–91. [PubMed: 10865104]
56. Fassbender C, Simoes-Franklin C, Murphy K, Hester R, Meaney J, Robertson IH, et al. The role of a right fronto-parietal network in cognitive control. Journal of Psychophysiology. 2006; 20:286–96.
57. Chambers CD, Bellgrove MA, Gould IC, English T, Garavan H, McNaught E, et al. Dissociable mechanisms of cognitive control in prefrontal and premotor cortex. J Neurophysiol. 2007; 98:3638–47. [PubMed: 17942624]
58. Chambers CD, Bellgrove MA, Stokes MG, Henderson TR, Garavan H, Robertson IH, et al. Executive “brake failure” following deactivation of human frontal lobe. Journal of Cognitive Neuroscience. 2006; 18:444–55. [PubMed: 16513008]
59. Chikazoe J, Konishi S, Asari T, Jimura K, Miyashita Y. Activation of right inferior frontal gyrus during response inhibition across response modalities. Journal of Cognitive Neuroscience. 2007; 19:69–80. [PubMed: 17214564]
60. Hirose S, Chikazoe J, Jimura K, Yamashita K, Miyashita Y, Konishi S. Sub-centimeter scale functional organization in human inferior frontal gyrus. Neuroimage. 2009; 47:442–50. [PubMed: 19442752]
61. Aron AR, Durston S, Eagle DM, Logan GD, Stinear CM, Stuphorn V. Converging evidence for a fronto-basal-ganglia network for inhibitory control of action and cognition. The Journal of Neuroscience. 2007; 27:11860–4. [PubMed: 17978025]
62. Aron AR, Poldrack RA. Cortical and subcortical contributions to stop signal response inhibition: Role of the subthalamic nucleus. The Journal of Neuroscience. 2006; 26:2424–33. [PubMed: 16510720]
63. Durston S, Thomas KM, Yang Y, Ulug AM, Zimmerman RD, Casey BJ. A neural basis for the development of inhibitory control. Dev Sci. 2002; 5:F9–F16.
64. Casey BJ, Castellanos FX, Giedd JE, Marsh WL, Hamburger SD, Schubert AB, et al. Implication of the right frontostriatal circuitry in response inhibition and attention-deficit/hyperactivity disorder. J Am Acad Child Adolesc Psychiatry. 1997; 36:374–83. [PubMed: 9055518]
65. Gauggel S, Rieger M, Feghoff TA. Inhibition of ongoing responses in patients with Parkinson’s disease. Journal of Neurology, Neurosurgery & Psychiatry. 2004; 75:539–44.
66. Rieger M, Gauggel S, Burmeister K. Inhibition of ongoing responses following frontal, nonfrontal, and basal ganglia lesions. Neuropsychology. 2003; 17:272–82. [PubMed: 12803433]
67. Thoma P, Koch B, Heyder K, Schwarz M, Daum I. Subcortical contributions to multitasking and response inhibition. Behav Brain Res. 2008; 194:214–22. [PubMed: 18692526]
68. MacDonald AW, Cohen JD, Stenger VA, Carter CS. Dissociating the role of the dorsolateral prefrontal and anterior cingulate cortex in cognitive control. Science. 2000; 288:1835–8. [PubMed: 10846167]
69. Cavanna AE. The precuneus and consciousness. CNS Spectrums. 2007; 12:545–52. [PubMed: 17603406]
70. Cavanna AE, Trimble MR. The precuneus: A review of its functional anatomy and behavioural correlates. Brain. 2006; 129:564–83. [PubMed: 16399806]

71. Shulman GL, Fiez JA, Corbetta M, Buckner RL, Miezin FM, Raichle ME, et al. Common blood flow changes across visual tasks: II. Decreases in cerebral cortex. Journal of Cognitive Neuroscience. 1997; 9:648–63. [PubMed: 23965122]

72. Wagner AD, Shannon BJ, Kahn I, Buckner RL. Parietal lobe contributions to episodic memory deficits. Trends Cogn Sci. 2005; 9:445–53. [PubMed: 16054861]

73. Aron AR. From reactive to proactive and selective control: Developing a richer model for stopping inappropriate responses. Biol Psychiatry. 2011; 69:55–68. [PubMed: 20970778]

74. Bokura H, Yamaguchi S, Kobayashi S. Electrophysiological correlates for response inhibition in a Go/NoGo task. Clinical Neurophysiology. 2001; 112:2224–32. [PubMed: 11738192]

75. Calhoun VD, Adali T, Pearlson GD, Kiehl KA. Neuronal chronometry of target detection: Fusion of hemodynamic and event-related potential data. Neuroimage. 2006; 30:544–53. [PubMed: 16246587]

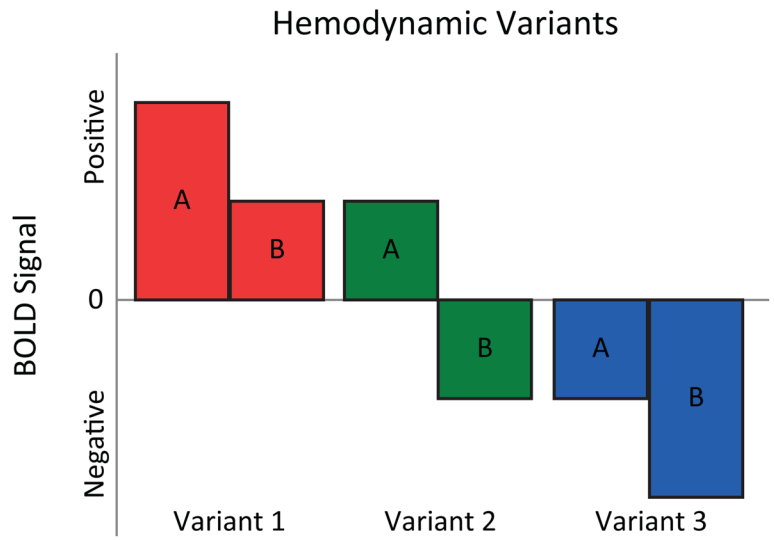

Figure 1.

The three possible hemodynamic variants in a traditional contrast of two conditions (i.e., A and B). Variant 1 (RED): condition A has as a large positive response relative to condition B's smaller response of the same direction; Variant 2 (GREEN): condition A has a positive response while condition B has a negative response; and Variant 3 (BLUE): condition A has a small negative response relative to condition B's large negative response. These three response types likely reflect different information processes in the brain and therefore highlight that not all interpretations of traditional contrasts are equal.

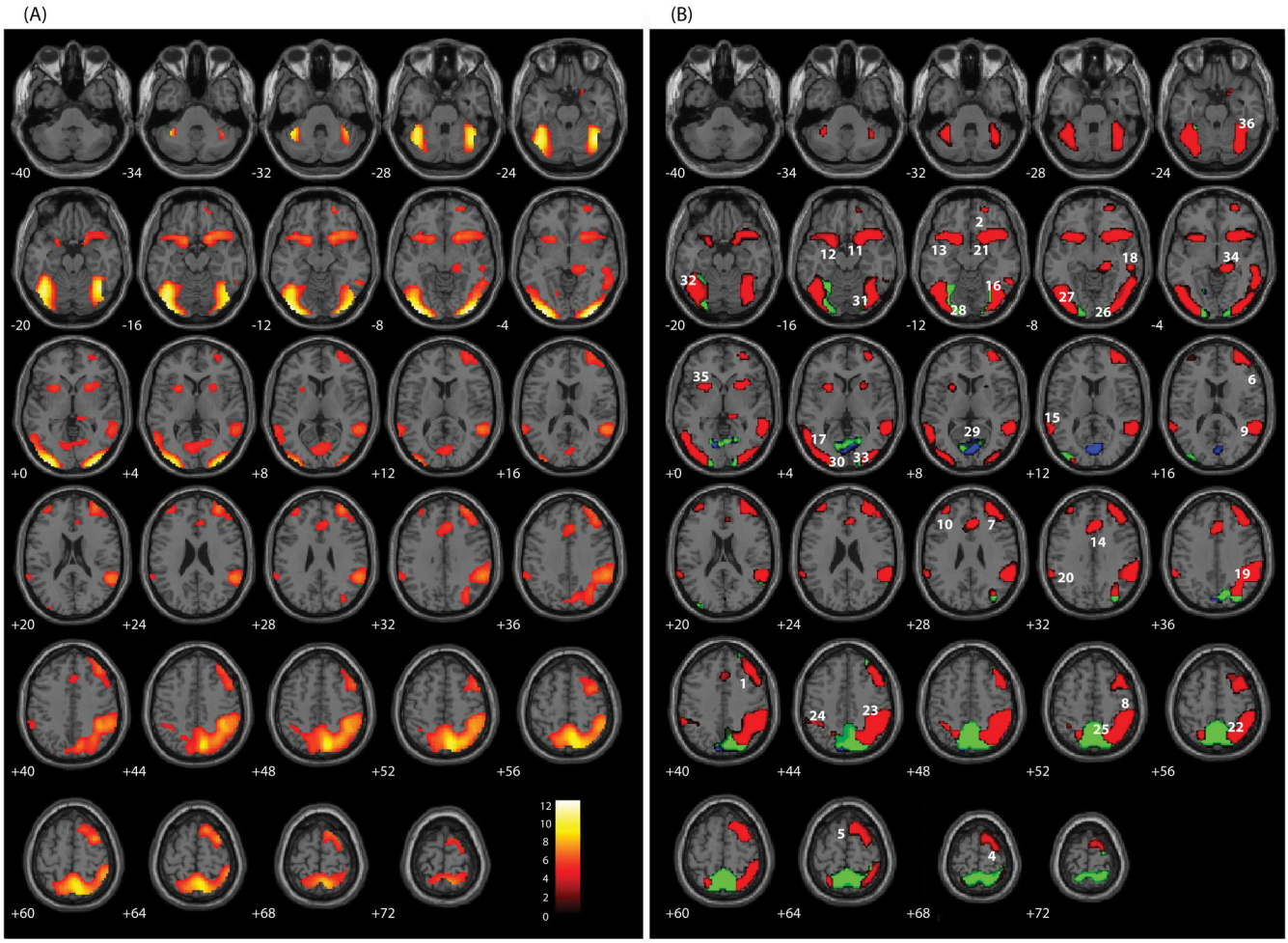

Figure 2.

(A) SPM axial slices of areas of significant activation ($p < .05$, corrected for multiple comparisons) for Correct Rejections (CR) relative to Hits from a traditional, omnibus analysis of 102 participants. (B) RED: CR has as a large positive response relative to the Hit condition's smaller response of the same direction. GREEN: CR has a positive response while Hits has a negative response. BLUE: CR has a small negative response relative to the Hit condition's large response of the same direction. Numeric labels denote significant regions of activation anatomically labeled in Table 2.

Table 1

general linear model-based fMRI analysis was used to analyze response inhibition in healthy adults
e size, baseline, and regions engaged during successful response inhibition across these 15 fMRI studies
ed.

FRONTAL			TEMPORAL				PARIETAL			OCCIPITAL			SUBCORTICAL			CEREBELLAR
ront Gy	Mid Front Gy	Inf Front Gy	Sup Temp Gy	Mid Temp Gy	Supra-mar Gy	Ins	Inf Par Lobe	Precun	Inf Occ Gy	Cuneus	Fusi-form Gy	Lingual Gy	Mid brain	Lenti Nuc	Cerebellum
x	x	x	x	x	x	x	x	x	x	x	x	x	x	x	x
x	x	x	x				x	x						x	x
x	x	x				x									
	x				x	x	x								
x	x					x	x	x						x	
x	x	x		x		x	x	x			x			x	x
x	x			x			x								x
x	x	x	x	x	x	x	x	x	x		x	x	x	x	x
x															x
	x	x		x		x	x								
x		x					x					x			

			FRONTAL				TEMPORAL			PARIETAL			OCCIPITA	
Publication	**Sample Size**	**Baseline**	**ACC**	**Sup Front Gy**	**Mid Front Gy**	**Inf Front Gy**	**Sup Temp Gy**	**Mid Temp Gy**	**Supra-mar Gy**	**Ins**	**Inf Par Lobe**	**Precun**	**Inf Occ Gy**	**Cuneus**
Liddle et al., 2001 (*p* < *.05*)	16	Implicit & Go trials	x	x	x	x	x	x	x		x	x	x	x
Braver et al., 2001 (*p* < *.05*)	14	Go trials	x		x	x		x			x	x		
Kiehl et al., 2000 (*p* < .001)	14	Implicit	x		x								x	
Garavan et al., 1999 (*p* < .001)	14	Go trials			x	x				x	x			

Table 2

Summary of the *t*-scores and the 36 regions of interest extracted from a traditional hemodynamic of Correct Rejections (CR) vs. Hits for the total sample (N = 102). 1-β ranges from .90 to 1.0. Using the hemodynamic variants, all regions identified in the traditional contrast exhibited a positive hemodynamic response of CR relative to a smaller positive response to Hits except for the cuneus, whose CR response was less negative than in Hits, and the precuneus, whose CR response was positive relative to a negative response in Hits. Eta squared is also presented as an account for BOLD signal variance assumed within each ROI.

		Total sample (n =102)					
	Location	***t*-score**	***x***	***y***	***z***	**BA**	η^2
	Frontal Lobe						
1	R Superior Frontal Gyrus	6.43****	39	36	39	9	.30
2	R Superior Frontal Gyrus	5.64***	21	57	−12	11	.24
3	R Superior Frontal Gyrus	4.48*	12	−3	75	6	.17
4	R Superior Frontal Gyrus	7.25****	15	18	66	6	.35
5	R Middle Frontal Gyrus	7.48****	33	6	63	6	.36
6	R Middle Frontal Gyrus	5.07**	48	48	15	10	.21
7	R Middle Frontal Gyrus	6.91****	33	51	27	10	.33
8	R Middle Frontal Gyrus	6.06***	48	12	51	8	.26
9	R Middle Frontal Gyrus	6.91****	54	−48	15	46	.33
10	L Middle Frontal Gyrus	5.16**	−33	51	27	10	.21
11	R Inferior Frontal Gyrus	6.75****	33	18	−15	47	.31
12	L Inferior Frontal Gyrus/Insula	6.78****	−18	12	−15	47	.32
13	L Inferior Frontal Gyrus	6.13****	−33	15	−12	13	.28
14	R Anterior Cingulate Cortex	5.55***	6	27	33	24	.24
	Temporal Lobe						
15	L Superior Temporal Gyrus	5.52***	−63	−48	12	22	.23
16	R Middle Temporal Gyrus	5.79***	57	−54	−12	37	.23
17	L Middle Temporal Lobe	5.76***	−57	−63	3	37	.24
18	R Middle Temporal Gyrus	5.08**	54	−30	−6	21	.20

		Total sample (n =102)					
	Location	***t*-score**	***x***	***y***	***z***	**BA**	η^2
19	R Supramarginal Gyrus	7.15****	57	−42	36	40	.34
20	L Supramarginal Gyrus	5.01**	−63	−45	33	40	.20
21	R Insula	6.97****	21	15	−15	13	.33
	Parietal Lobe						
22	R Inferior Parietal Lobule	7.48****	48	−45	57	40	.36
23	R Inferior Parietal Lobule	8.16****	39	−42	45	40	.40
24	L Inferior Parietal Lobule	4.70*	−36	−48	45	40	.19
25	R Precuneus	10.18****	9	−69	54	7	.50
	Occipital Lobe						
26	R Inferior Occipital Gyrus	12.34****	36	−93	−6	18	.61
27	L Inferior Occipital Gyrus	11.69****	−36	−93	−6	18	.57
28	L Inferior Occipital Gyrus	11.55****	−39	−90	−12	18	.57
29	R Cuneus	5.33**	6	−69	6	30	.23
30	L Cuneus	5.43**	−6	−75	6	30	.23
31	R Fusiform Gyrus	9.16****	45	−75	−15	19	.45
32	L Fusiform Gyrus	11.53****	−42	−66	−18	19	.57
33	R Lingual Gyrus	5.16**	18	−66	3	18	.21
	Subcortical						
34	R Midbrain	5.44**	18	−30	−3	NA	.22
35	L Putamen	5.68***	−24	12	0	NA	.25
	Cerebellum						
36	R Cerebellum (Declive)	11.14****	39	−57	−24	NA	.54

* = $p \leq .05$;

** = $p \leq .01$;

*** = $p \leq .001$;

**** = $p \leq .0001$ corrected for multiple comparisons.

Behav Brain Res. Author manuscript; available in PMC 2015 May 19.

Table 3

Summary of regions extracted to represent the three hemodynamic variants. The number of voxels and peak voxel within each region is presented. The beta weights for Correct Rejection (CR) and Hits are presented to highlight the relative increase or decrease from baseline for each condition in each region.

		Total sample (n =102)					
	Location	***Voxels***	***x***	***y***	***z***	***CR Beta***	***Hit Beta***
	Variant 1						
1	R Hippocampus	76	17	−30	−5	0.6430	.01299
2	L Puteman	269	−26	12	−9	0.8225	0.3518
3	R Insula	488	32	15	−11	1.0178	0.4000
4	R Middle Frontal Gyrus	1029	32	31	39	0.8317	0.3100
5	R Cingulate	145	3	26	32	0.8871	0.3087
6	L Middle Frontal Gyrus	63	−34	51	25	0.6258	0.1347
7	L Sub-Gyral	1340	−41	−66	−2	0.8271	0.2079
8	R Superior Temporal Gyrus	2710	43	−55	32	0.9253	0.2825
	Variant 2						
9	R Cuneus	52	19	−97	−4	0.2996	−0.2092
10	R Fusiform Gyrus	3	31	−52	−15	0.3687	−0.0320
11	R Fusiform Gyrus	1	33	−45	−18	0.3814	−0.0020
12	L Lingual Gyrus	223	−25	−78	−13	0.3855	−0.1287
13	R Lingual Gyrus	23	29	−73	−13	0.3964	−0.0424
14	R Middle Frontal Gyrus	1	27	66	9	0.5723	−0.0023
15	L Middle Occipital Gyrus	31	−36	−89	15	0.2795	−0.0943
16	R Parahippocampal Gyrus	4	17	−38	−5	0.4649	−0.0435
17	R Posterior Cingulate	91	1	−71	4	0.0369	−0.5023
18	R Precuneus	1368	5	−62	55	0.4935	−0.3027
19	R Superior Frontal Gyrus	21	30	43	43	0.4392	−0.0509
20	R Superior Frontal Gyrus	6	26	−10	71	0.3584	−0.0496
21	R Superior Frontal Gyrus	2	16	57	−14	0.4520	−0.0408
22	R Supramarginal Gyrus	8	57	−57	21	0.5117	−0.0138
	Variant 3						

		Total sample (n = 102)					
	Location	***Voxels***	***x***	***y***	***z***	***CR Beta***	***Hit Beta***
23	L Lingual Gyrus	3	−13	−96	−5	−0.0281	−0.3886
24	R Cuneus	3	14	−95	−2	−0.0365	−0.4378
25	R Cuneus	149	2	−76	8	−0.0407	−0.5836
26	L Precunues	32	−3	−82	41	−0.0803	−0.6936